



Bisaryldiketene derivatives: A new class of selective ligands for *c-myc* G-quadruplex DNA

Dan Peng, Jia-Heng Tan, Shuo-Bin Chen, Tian-Miao Ou, Lian-Quan Gu, Zhi-Shu Huang*

School of Pharmaceutical Sciences, Sun Yat-Sen University, Guangzhou 510006, People's Republic of China

ARTICLE INFO

Article history:

Received 7 August 2010

Revised 5 October 2010

Accepted 5 October 2010

Available online 28 October 2010

Keywords:

G-quadruplex DNA

Bisaryldiketene derivatives

Ligand–quadruplex interactions

Selectivity

ABSTRACT

A series of bisaryldiketene derivatives were designed and synthesized as a new class of specific G-quadruplex ligands. The ligand–quadruplex interactions were further evaluated by FRET, ITC, and PCR stop assay. In contrast to most of the G-quadruplex ligands reported so far, which comprise an extended aromatic ring, these compounds are neither polycyclic nor macrocyclic, but have a non-aromatic and relative flexible linker between two quinoline moieties enabling the conformation of compounds to be flexible. Our results showed that these bisaryldiketene derivatives could selectively recognize G-quadruplex DNA rather than binding to duplex DNA. Moreover, they showed promising discrimination between different G-quadruplex DNA. The primary binding affinity of ligand **M2** for *c-myc* G-quadruplex DNA was over 200 times larger than that for telomere G-quadruplex DNA.

© 2010 Elsevier Ltd. All rights reserved.

1. Introduction

Guanine-rich single strand can adopt higher-order and functionally useful structures called the G-quadruplexes.^{1–3} The building blocks of G-quadruplexes are the G-quartets, which stack up with one on top of another to form such secondary DNA structures.⁴ G-quadruplexes are widely dispersed in eukaryotic genomes, including telomeric DNA,⁵ immunoglobulin switch regions,⁶ rDNA,⁷ and series of gene promoter regions, such as *c-myc*,⁸ *c-kit*,⁹ *bcl-2*,¹⁰ *VEGF*,¹¹ and so on.^{12,13} These structures are diverse showing distinct strand stoichiometry, strand directivity as well as loop and groove configuration.¹⁴

As G-quadruplexes are widely found throughout human genome, they are thought to play important role in some biological events.¹⁵ For example, telomere is of great importance in the regulation of cellular proliferation.¹⁶ The guanine-rich repeats of the telomeric single-stranded overhang can be elongated by telomerase, an enzyme not found in most normal somatic cells, but present in 85–90% of cancer cells contributing to their immortality.^{17,18} Ligands capable of inducing and stabilizing G-quadruplex formation of these telomeric DNA could inhibit telomerase activity and interference with telomere biology.^{19,20} On the other hand, *c-myc* is an important proto-oncogene involved in cellular proliferation and cell growth. The nuclear hypersensitivity element III₁, upstream of the P1 promoter of *c-myc*, controls 80–90% of the *c-myc* transcription level.^{21,22} This guanine-rich sequence can form intramolecular G-quadruplex structures and further function as a

transcriptional repressor element.^{23,24} Ligands binding and stabilizing such G-quadruplex DNA could effectively inhibit the transcription activity of *c-myc*.^{25,26} Thus, G-quadruplex ligands have potential as anti-cancer agents that act by interference with telomere maintenance or by alteration of oncogene expression levels.^{27,28} However, further efforts in appropriate drug design are needed to control the G-quadruplex selectivity over duplex DNA because ligand interaction with duplex DNA leads to acute toxic and intolerable side effects on normal tissues. With an increasing number of G-quadruplexes identified in the genome, ligand design has also been directed at selectivity among different G-quadruplex species.^{29,30}

Several small molecules have been identified to bind and stabilize G-quadruplexes, which subsequently inhibit telomerase activity, shorten the telomere length or down-regulate oncogene expression. Most of them comprise a planar, aromatic core.^{29,30} Examples include polyaromatic hydrocarbons and macrocyclic frameworks.^{31,32} Besides these compounds, some flexible ligands with unfused aromatic scaffold have aroused wide interest recently because of their excellent quadruplex:duplex selectivity and also promising discrimination between intramolecular G-quadruplexes.^{33,34} Compounds **12459**,³⁵ **Bipy-1b**,³⁶ and **307A**,³⁷ are a kind of unfused aromatic molecules, which all possessing two methylated quinoline (quinolinium) side arms connected by different central aromatic linkers (Fig. 1). The carbon–nitrogen single bond in **12459** and **Bipy-1b** or amido bond in **307A** could partially rotate so that the whole molecules are not entirely planar, which prevent the ligands from intercalating into duplex DNA but still fit for the G-quartet. Accordingly, these compounds display good G-quadruplex selectivity over duplex DNA.

* Corresponding author. Tel./fax: +86 20 39943056.

E-mail address: ceshzs@mail.sysu.edu.cn (Z.-S. Huang).

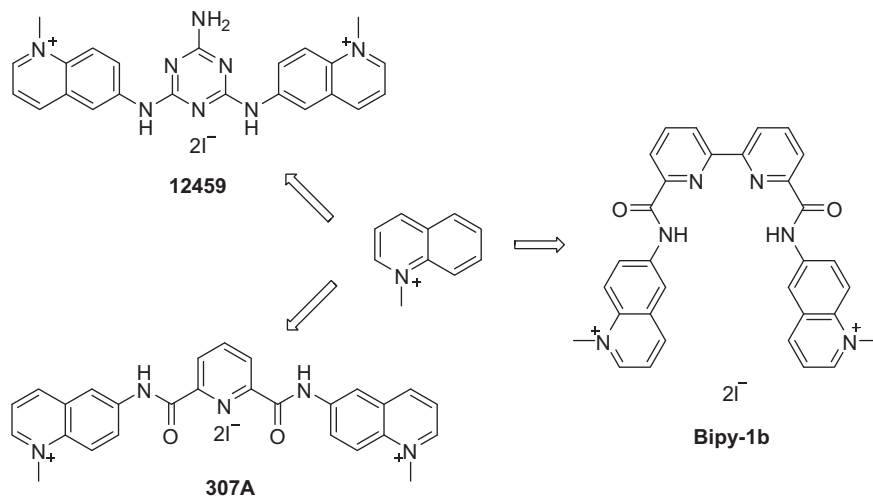


Figure 1. The structures of ligand **12459**, **Bipy-1b**, and **307A**.

In this study, in view of the tempting G-quadruplex selectivity exhibited by **12459**, **Bipy-1b**, and **307A**, we retained the bisquinolinium moiety which is the common pharmacophore of these three ligands and synthesized a series of bisaryldiketene derivatives with more flexible frameworks as central linkers. Our aim is to find whether such modification would enhance the selectivity of these derivatives for G-quadruplex with respect to duplex DNA and also selectivity between different G-quadruplex DNA. Furthermore, some derivatives with substitution of quinoline ring were also involved in the activity tests to probe the essentiality of N-methylated modification. In subsequent activity tests, we investigated the stabilization ability and selectivity of these derivatives using fluorescence resonance energy transfer (FRET) melting experiment. Their binding affinity to various G-quadruplex was further determined by isothermal titration calorimetry (ITC) experiment. Ultimately we analyzed the biological function of the derivatives using polymerase chain reaction stop assay (PCR stop assay).

2. Results and discussion

2.1. Synthesis of bisaryldiketene derivatives

The facile synthetic pathway for bisaryldiketene derivatives was shown in Scheme 1. Treatment of 6-methylquinoline with SeO_2 produced 6-formylquinoline. Compounds **1–4** were then synthesized by aldol reaction between 6-formylquinoline and various ketones for 10–30 min.³⁸ Further suspension of compounds **1–4** in excess methyl iodide provided derivatives **M1–M4**. Finally, the configuration of all target compounds was confirmed by the NOESY analysis (Supplementary data). As shown in Scheme 1, results indicated that most of bisaryldiketene derivatives showed linear shaped (*E,E*) configuration with the exception of **3** and **M3** adopting U-shaped (*Z,Z*) configuration. The (*Z,Z*) configuration was the most stable conformation for **3** and **M3**, and we could not obtain their (*E,E*) isomers at present.

2.2. FRET-melting studies of bisaryldiketene derivatives

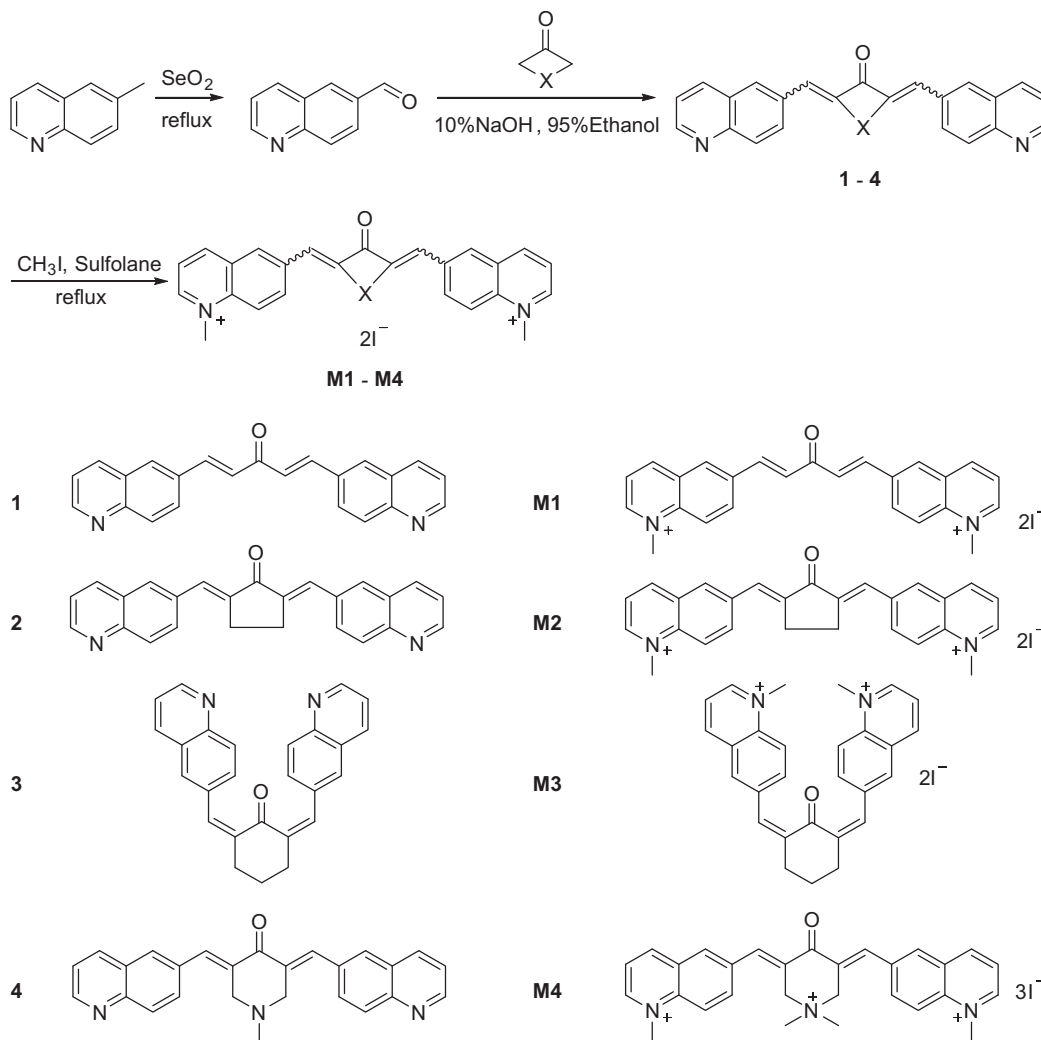
To evaluate the stabilization and selectivity of bisaryldiketene derivatives for G-quadruplex DNA, FRET-melting experiments were carried out. The human telomeric G-quadruplex DNA (F21T) and three oncogene promoter G-quadruplexes *c-myc* (F22T), *c-kit1* (F-c-kit1-T), and *c-kit2* (F-c-kit2-T) containing fluorophores at both 5'-end and 3'-end were used in this assay. A

sequence that forms hairpin duplex DNA structure F10T as a non-quadruplex control was also involved.^{39–41} The primary structures of all oligomers used in this study were shown in Table 4. The melting temperature of all G-quadruplexes was determined in the presence of 1 μM of bisaryldiketene derivatives in Tris-HCl buffer containing 60 mM KCl. The result of FRET-melting assay was represented as enhanced melting temperature (ΔT_m) reported in Table 1.

As shown in Table 1, most derivatives could stabilize all the G-quadruplexes. It was clear that **M2** could raise the melting temperatures of four G-quadruplexes most greatly by about 17–29 °C, and **M1** increased the melting temperatures of four G-quadruplexes by about 13–24 °C, indicating their excellent stabilization effects on tested G-quadruplexes. Stabilization effects of **M3** and **M4** on G-quadruplexes were weaker than that of **M1** and **M2**, with ΔT_m values of 8–16 °C. Moreover, **M1–M4** showed much better stabilizing ability than derivatives **1–4**. As could be seen from Table 1, ΔT_m values of **1–4** for all the G-quadruplexes were about 0–5 °C.

Comparison of these FRET assay results revealed that introduction of the positive charges by methylation at nitrogen position of quinoline ring significantly improved the interaction of ligand with G-quadruplex structure. The inducement might be their enhanced electrostatic interactions with the negative backbone and ion channel. Nevertheless, it was interesting to find compound **M4** with three protonated centers showed the worst stabilization ability among quinolinium compounds. This result indicated that the charge distribution of such compounds was not very favorable for the interactions with G-quadruplexes. Accordingly, the essential point for further G-quadruplex ligand design should consider how to introduce appropriate number and configuration of positive charge to the scaffold. Besides, compounds **M1** and **M2** with linear shaped configuration exhibited stronger stabilization potential for all the tested G-quadruplexes than U-shaped compound **M3**, showing the geometric configuration of bisaryldiketene derivatives might be another influence factor for ligand–quadruplex recognition.

On the other hand, it was quite evident that all the studied ligands could barely stabilize the hairpin structure formed by F10T with ΔT_m values of 0 or 1 °C, suggesting their poor binding to the duplex DNA.^{42,43} However, it should be also emphasized that the selectivity among different G-quadruplex species could not be well determined at this stage because the ligands seemed to have potential to stabilize all the different G-quadruplex species.³⁴



Scheme 1. Synthesis of bisaryldiketene derivatives.

Table 1
Stabilization temperatures (ΔT_m) determined by FRET-melting experiment^a

Ligand	F22T ^b	F21T ^b	F-c-kit1-T ^b	F-c-kit2-T ^b	F10T ^b
1	2	3	10	5	0
2	2	0	1	0	0
3	2	0	1	0	0
4	1	4	1	1	0
M1	13	17	24	17	0
M2	17	23	29	20	1
M3	9	10	17	12	0
M4	7	7	14	6	0

^a $\Delta T_m = T_m(\text{DNA} + \text{ligand}) - T_m(\text{DNA})$. In the absence of ligand, T_m values of annealed F22T, F21T, F-c-kit1-T, F-c-kit2-T, and F10T are 78, 60, 54, 75, and 64 °C, respectively.

^b The primary structures of all oligomers used in this study were shown in Table 4.

To further characterize the selectivity of these ligands for G-quadruplexes, competitive FRET experiment was employed. Excess duplex DNA ds26 was mixed with *c-myc* G-quadruplex F22T before committed to FRET-melting assay with ligands for ΔT_m values determination.³⁶ The result of competitive FRET-melting assay was plotted in Figure 2. From Figure 2 we observed no or slight decrease of ΔT_m values caused by the addition of massive duplex competitor ds26, which indicated that tested compounds could specifically stabilize *c-myc* G-quadruplex structure with discrimi-

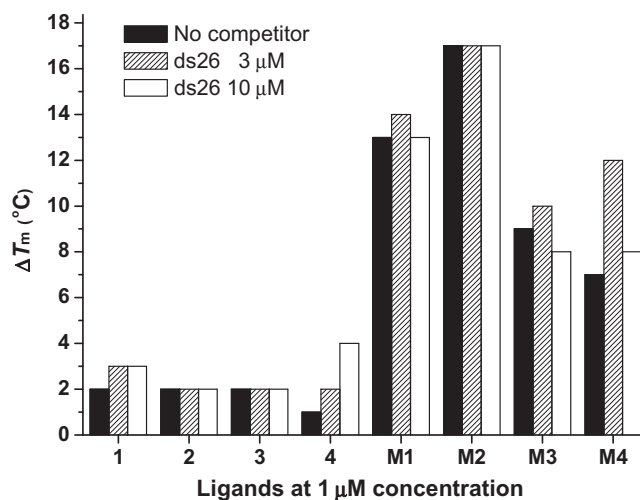


Figure 2. Competitive FRET results for 1 μM of compounds in 0.2 μM F22T without or with 3 μM or 10 μM of duplex DNA competitor ds26.

nation against duplex DNA. Moreover, this competitive FRET experiment was also used to estimate the ligand's selectivity between different G-quadruplexes. In the assay, the most promising

compound **M2** and non-fluorescent DNA competitor c-kit1 (*c-kit1* G-quadruplex DNA), c-kit2 (*c-kit2* G-quadruplex DNA) as well as HTG21 (telomeric G-quadruplex DNA) was employed.⁴⁴ As shown in Figure 3, the thermal stabilization of F22T enhanced by **M2** was slightly affected in the presence of competitor HTG21. And such stabilizing ability was also retained at around 40% even with the addition of 10 μM (50-fold) G-quadruplex competitor c-kit1 and c-kit2. Accordingly, the combined results of these assays demonstrated that bisaryldiketene derivative **M2** could be considered as a new class of selective G-quadruplex ligands showing binding preference for *c-myc* G-quadruplex DNA.

2.3. ITC studies of bisaryldiketene derivatives

To gain more details on the binding affinity and selectivity of bisaryldiketene derivatives for different G-quadruplex species, ITC experiments, a valuable method aimed at characterizing the energetics of molecular interactions, were performed.^{45–47}

The titrations to G-quadruplexes were carried out on ligand **M2** that showing the best stabilization effect in FRET-melting experiment. All G-quadruplex DNA and **M2** were dissolved in a 10 mM Tris–HCl buffer containing 150 mM KCl. Representative titration curves along with corresponding enthalpy values were presented in Figure 4, where small aliquots of **M2** solution were added from the syringe into the microcalorimeter cell containing G-quadruplexes. We also carried out dilution control experiments, namely ligand dilution (where same **M2** solution was added from the syringe into 10 mM Tris–HCl buffer containing 150 mM potassium without G-quadruplexes in the cell). We observed that the enthalpy change for ligand dilution was typically quite small in magnitude. The resulting net enthalpy change was then determined by subtracting the dilution control.

Analyzing the thermograms of **M2** titrated to various G-quadruplexes in Figure 4, it was apparent that the curve of **M2** titrated to Pu27 (*c-myc* G-quadruplex DNA) exhibited the presence of at least two independent binding processes,⁴⁸ while that of **M2** titrated to c-kit1 and c-kit2 exhibited similar one binding process.⁴⁹ From the thermogram of **M2** titrated to HTG21, a much smaller enthalpy change in magnitude implied a much weaker interaction between **M2** and HTG21. As the concentration of G-quadruplexes and **M2** were accurately known, fit the thermograms with two sites model for Pu27, and one site model for c-kit1, c-kit2, and HTG21, we could calculate average enthalpy change ΔH , binding constant K , and stoichiometry n . Furthermore, since temperature (T) is held constant throughout the entire experiment, the free energy (ΔG)

and the change in entropy (ΔS) could also be determined, as shown in Table 2.

From Table 2, we learnt that the primary binding constants K were 8.05×10^6 for Pu27, 3.08×10^5 for c-kit1, 1.27×10^5 for c-kit2, and 3.61×10^4 for HTG21, respectively. It is obviously that ligand **M2** possessed very strong interaction with *c-myc* G-quadruplex DNA with the primary binding affinity almost 25 times larger than that with *c-kit* G-quadruplex DNA and 200 times larger than that with telomeric G-quadruplex DNA. These findings were in parallel with above competitive FRET experiment. Thus, **M2** could be considered as an excellent selective G-quadruplex ligand, not only between G-quadruplex and duplex, but also between various G-quadruplexes.

To disclose the driven force of the physical processes involved in the binding reaction, we compared the thermodynamic parameters ΔH , $-\Delta S$ and ΔG during the processes that **M2** titrated to different G-quadruplex DNA, as shown in Figure 5. First of all, the negative values of ΔG for all G-quadruplexes indicated that interaction between **M2** and all the G-quadruplexes took place spontaneously. Interactions between **M2** and the Pu27, c-kit1, and c-kit2 G-quadruplexes were enthalpically driven, being that the corresponding ΔH values were higher than $-\Delta S$ values. These data indicated that enthalpic interactions including hydrogen bond formation, charge interactions, and van der Waal's interactions were favorable during these ligand–quadruplex binding processes. In contrast, a small positive ΔH as well as large negative $-\Delta S$ values found in **M2**–HTG21 binding process indicated the entropically favorable binding and suggested that hydrophobic interactions were the main driving force.^{47,50}

These driven force diversity might due to the secondary structures variance between these four G-quadruplexes. The *c-myc*, *c-kit1*, and *c-kit2* sequence fold into parallel G-quadruplex structures in a KCl containing buffer whereas telomeric sequence forms hybrid G-quadruplex structure. Even though *c-kit1* and *c-kit2* sequences form parallel G-quadruplexes as *c-myc* sequence, they show extinct variance in loops, such as loop numbers, loop constitution, and the bases that form a loop.^{1,3,51} Compound **M2** is neither polycyclic nor macrocyclic. It has flexible aliphatic five-member ring in the middle core and free rotation around the double bond that would enable the adoption of possible twisted and co-planar conformations. Hence, owing to such conformational flexibility, we perceived ligand **M2** would offer the potential for modes of G-quadruplex recognition (such as loop or groove interactions) other than the more typical G-quartet binding site.⁵² That the loop and groove regions varied from different G-quadruplex species might be the important reason where the different G-quadruplexes selectivity of the ligand comes from.⁵³

2.4. Inhibition of amplification in the promoter region of *c-myc* by bisaryldiketene derivatives

To further study the induction of biologically relevant G-quadruplex formation by the bisaryldiketene derivatives, PCR stop assay was carried out.^{54,55} Herein we performed the evaluation on *c-myc* G-quadruplex Pu27 which had best binding affinity with ligand as revealed in above ITC studies. In the presence of the derivatives, the single-strand Pu27 was folded into a G-quadruplex structure and blocked the hybridization with its complementary strand. In that case, 5' to 3' primer extension by DNA *Taq* polymerase was arrested and the final double-stranded DNA PCR product could not be detected by electrophoresis separation.⁵⁶ Concentrations of all the ligands that inhibited amplification by 50% (IC_{50}) were listed in Table 3. The derivatives with higher stabilizing potential of G-quadruplex structure were in general better stabilizing inhibitors of amplification in Pu27. Compounds **M1–M4** which had positive charges were much more effective than those without positive charges.

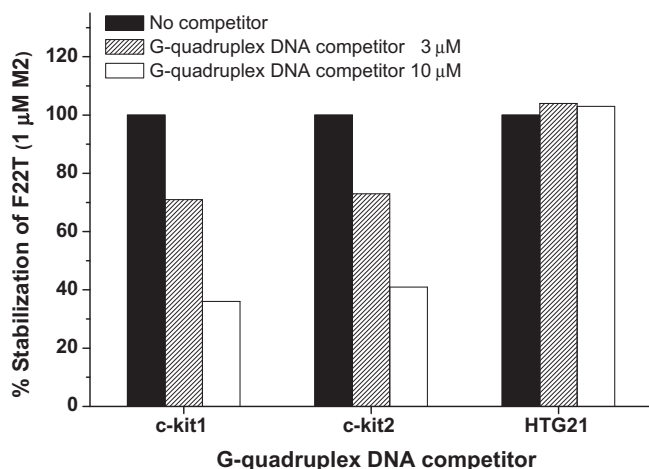


Figure 3. Competitive FRET results for 1 μM of compound **M2** in 0.2 μM F22T without or with 3 μM or 10 μM of G-quadruplex DNA competitor c-kit1, c-kit2, and HTG21.

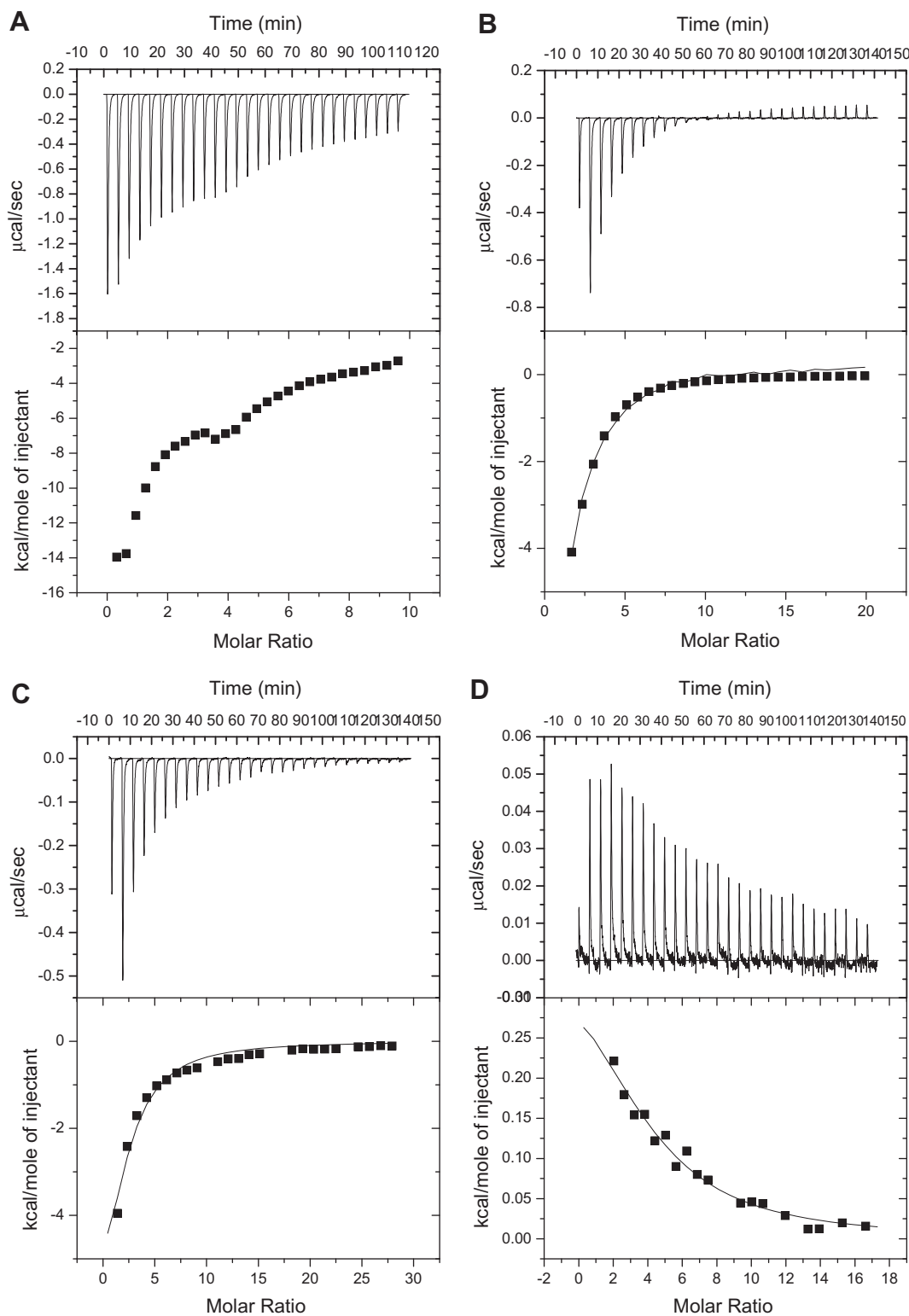


Figure 4. Compound **M2** titrated to 5 μM Pu27 (A), c-kit1 (B), c-kit2 (C), and HTG21 (D) in 10 mM Tris–HCl buffer, pH 7.4 with 150 mM KCl.

M1–M3 showed excellent inhibitory effect with very low IC_{50} of 0.7–1.1 μM . These results were correlated to the ΔT_m values in Table 1.

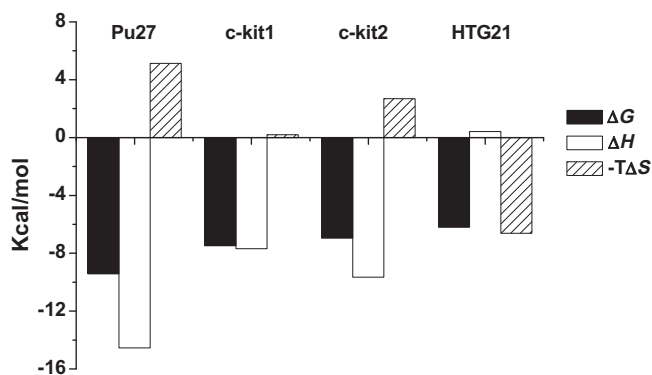
3. Conclusions

A new class of bisaryldiketene derivatives were designed and synthesized by a facile method. Their interaction with the different

G-quadruplex DNA had been investigated in detail. Our results demonstrated that bisaryldiketene derivatives could bind and stabilize G-quadruplex structures. Introducing positive charges to bisaryldiketene derivatives effectively improves their interaction with G-quadruplexes and increases the inhibitory effect on the hybridization. With two bisquinoline or bisquinolinium moieties connected with a flexible diketene group, these unused aromatic derivatives selectively bound to G-quadruplexes rather than du-

Table 2The Gibbs energy (ΔG), enthalpy change (ΔH), entropy change (ΔS), binding constants (K), and binding ratio (n) of **M2** obtained in ITC experiment

DNA	n	K (M^{-1})	ΔH (cal mol $^{-1}$)	ΔS (cal mol $^{-1}$ K $^{-1}$)	ΔG (cal mol $^{-1}$)
Pu27	0.879	8.05×10^6	-1.455×10^4	-17.2	-9421.82
	6.17	4.42×10^4	-1.227×10^4	-19.9	-6336.815
c-kit1	2.12	3.08×10^5	-7691	-0.675	-7489.74875
c-kit2	1.95	1.27×10^5	-9653	-9.02	-6963.687
HTG21	4.18	3.61×10^4	416.3	22.2	-6202.63

**Figure 5.** The Gibbs energy (ΔG), enthalpy change (ΔH), and entropy change ($-T\Delta S$) during the interactions between **M2** and different G-quadruplex DNA.**Table 3**IC₅₀ values determined by the PCR stop assay

Compounds	1	2	3	4	M1	M2	M3	M4
IC ₅₀ (μM)	>20	>20	>20	>20	0.7	0.9	1.1	12.6

plex DNA. Moreover, derivative **M2** showed more than 200 times selectivity for *c-myc* G-quadruplex DNA over telomeric G-quadruplex DNA. Further energetic analysis showed that this promising selectivity might arise from the different binding mode and shape matching of **M2** during its interactions with different G-quadruplex DNA. Regarding our initial effort has succeeded to enhance ligands' selectivity between different G-quadruplex DNA, more detailed investigations on the biophysics and pharmacology of these compounds are now underway.

4. Experimental

4.1. General

Commercially available chemicals and solvents were used without further purification, unless otherwise stated. NMR was recorded on a Bruker AvanceIII 400 spectrometer whereas TMS (δ 0 ppm) was used as an internal standard for spectra

Table 4Oligomers used in the present study^{39–41,54}

Oligomer	Sequence	Description
F22T	5'-FAM-d[TGAG ₃ TG ₃ TAG ₃ TG ₃ TA ₂]-TAMRA-3'	Fluorescent-labeled <i>c-myc</i> sequence
F21T	5'-FAM-d[G ₃ (T ₂ AG ₃) ₃]-TAMRA-3'	Fluorescent-labeled telomeric sequence
F-c-kit1-T	5'-FAM-d [G ₃ AG ₃ CGCTG ₃ AGGAG ₃]-TAMRA-3'	Fluorescent-labeled c-kit1 sequence
F-c-kit2-T	5'-FAM-d[G ₃ CG ₃ CGCGAG ₃ AG ₄]-TAMRA-3'	Fluorescent-labeled c-kit2 sequence
F10T	5'-FAM-d[TATAGCTATA-HEG-TATAGCTATA]-TAMRA-3', HEG is [(-CH ₂ -CH ₂ -O-)] ₆	Fluorescent-labeled hairpin duplex DNA
ds26	5'-d[CA ₂ TCC ₂ ATCGA ₂ T ₂ CGATC ₂ GAT ₂ G]-3'	Duplex DNA
Pu27	5'-d[TG ₄ AG ₃ TG ₄ AG ₃ TG ₄ A ₂ G ₂]-3'	<i>C-myc</i> sequence
c-kit1	5'-d[G ₃ AG ₃ CGCTG ₃ AGGAG ₃]-3'	<i>C-kit1</i> sequence
c-kit2	5'-d[G ₃ CG ₃ CGCGAG ₃ AG ₄]-3'	<i>C-kit2</i> sequence
HTG21	5'-d[G ₃ (T ₂ AG ₃) ₃]-3'	Telomeric sequence
Pu27 _{rev}	5'-d[ATCGATCGCTTCTCGTCTTCCCCA]-3'	Complementary sequence used in PCR stop assay

recorded. HRMS was recorded on an Agilent Ion-TOF-LC/MC spectrometer.

All oligomers/primers used in this study were purchased from Invitrogen (China) and Sangon (China) as shown in Table 4. Before usage, they were diluted from stock (100 μM) to the correct concentrations in relevant KCl containing buffer and then annealed by heating to 90 °C for 5 min, gradually cooled to room temperature, and incubated at 4 °C overnight to ensure the formation of G-quadruplex structure. Acrylamide/bisacrylamide solution and *N,N,N',N'*-tetramethyl-ethylenediamine were purchased from Sigma. Stock solutions of all the derivatives (10 mM) were made using DMSO. Further dilutions to working concentrations were made with relevant buffer immediately prior to use.

4.2. 6-Formylquinoline

6-Methylquinoline (10 g, 65.4 mmol) was firstly heated to 160 °C, and followed by the addition of SeO₂ powder (15.0 g, 87.0 mmol). This mixture was refluxed for 12 h and then cooled to room temperature. After pouring out the upper solution, the residue was extracted with massive amount of ethyl acetate until TLC detection showed there was no product left. The combined organic phase was evaporated and purified by gel column with petroleum ether/ethyl acetate (9:1) elution to afford a pale yellow powder (5.3 g, 53%).

4.3. (1E,4E)-1,5-Di-(quinolin-6-yl)-penta-1,4-dien-3-one (1)

To a stirred solution of 6-formylquinoline (1.02 g, 10 mmol) and acetone (360 μL , 5 mmol) in 8 mL 95% ethanol, 3 mL 10% NaOH aqueous solution was added dropwise at room temperature and the mixture was stirred for further 20 min. The precipitate was then separated from solvent by filtration and rinsed with water to afford a yellow solid **1** (0.88 g, 85%). Mp 155–156 °C; ¹H NMR (400 MHz, DMSO-*d*₆) δ 8.96 (s, 2H), 8.52–8.20 (m, 6H), 8.06 (dd, 4H, $J = 24.6, 12.3$), 7.58 (d, 4H, $J = 15.9$). ESI-HRMS m/z : calcd for C₂₃H₁₆N₂O [M+H]⁺ 337.1296, found 337.1337.

4.4. (2E,5E)-2,5-Bis-(quinolin-6-ylmethylene)-cyclopentanone (2)

Following the method for production of **1**, a yellow solid **2** (0.75 g, 67%) was obtained. Mp 153–154 °C; ¹H NMR (400 MHz,

DMSO-*d*₆) δ 9.06 (d, 2H, *J* = 3.6), 8.69 (d, 2H, *J* = 8.1), 8.43 (s, 2H), 8.20 (dd, 4H, *J* = 19.8, 9.1), 7.79–7.72 (m, 2H), 7.69 (s, 2H), 3.32 (s, 4H). ESI-HRMS *m/z*: calcd for C₂₅H₁₈N₂O [M+H]⁺ 363.1497, found 363.1501.

4.5. (2Z,6Z)-2,6-Bis-(quinolin-6-ylmethylene)-cyclohexanone (3)

Following the method for production of **1**, a yellow solid **3** (0.86 g, 65%) was obtained. Mp 155–158 °C; ¹H NMR (400 MHz, CDCl₃) δ 8.86 (dd, 2H, *J* = 4.1, 1.3), 8.11 (d, 2H, *J* = 7.8), 8.05 (d, 2H, *J* = 8.8), 7.90 (s, 2H), 7.83 (s, 2H), 7.75 (dd, 2H, *J* = 8.8, 1.7), 7.36 (dd, 2H, *J* = 8.3, 4.2), 3.03–2.93 (m, 4H), 1.85–1.74 (m, 2H). ¹³C NMR (101 MHz, CDCl₃) δ 188.90, 150.16, 146.86, 136.04, 135.35, 135.30, 133.22, 130.18, 128.88, 128.51, 127.00, 120.64, 27.54, 21.91. ESI-HRMS *m/z*: calcd for C₂₆H₂₀N₂O [M+H]⁺ 377.1654, found 377.1649.

4.6. (3E,5E)-1-Methyl-3,5-bis-(quinolin-6-ylmethylene)-piperidin-4-one (4)

Following the method for production of **1**, a yellow solid **4** (0.92 g, 74%) was obtained. Mp 168–171 °C; ¹H NMR (400 MHz, CDCl₃) δ 8.95 (dd, 2H, *J* = 4.2, 1.7), 8.23 (s, 1H), 8.20 (s, 1H), 8.16 (s, 1H), 8.13 (s, 1H), 8.00 (s, 2H), 7.85 (d, 2H, *J* = 1.7), 7.77 (d, 1H, *J* = 2.0), 7.74 (d, 1H, *J* = 2.0), 7.47 (d, 1H, *J* = 4.2), 7.44 (d, 1H, *J* = 4.2), 3.92 (d, 4H, *J* = 1.6), 2.52 (s, 3H). ESI-HRMS *m/z*: calcd for C₂₆H₂₁N₃O [M+H]⁺ 392.1763, found 392.1770.

4.7. 6,6'-((1E,4E)-3-Oxopenta-1,4-diene-1,5-diyl)-bis-(1-methylquinolinium) iodide (M1)

Compound **1** (40 mg, 0.12 mmol) was heated to 120 °C in 2.5 mL sulfolane, and excess CH₃I (0.2 g, 1.19 mmol) was added. The mixture was refluxed for 4 h, and orange solid precipitated. After cooling to room temperature, the precipitate was separated from solvent by filtration and rinsed with ethyl ether to afford an orange solid **M1** (58 mg, 79%). Mp >300 °C; ¹H NMR (400 MHz, D₂O) δ 9.14 (s, 4H), 8.54 (s, 4H), 8.40 (s, 2H), 7.99 (d, 4H, *J* = 10.9), 7.50 (d, 2H, *J* = 15.2), 4.61 (s, 6H). ¹³C NMR (101 MHz, DMSO) δ 188.42, 150.58, 147.18, 140.48, 138.98, 135.86, 133.65, 130.72, 129.44, 129.16, 122.83, 120.08, 45.50. ESI-HRMS *m/z*: calcd for C₂₅H₂₂N₂O [M–2I]²⁺ 183.0866, found 183.0863.

4.8. 6,6'-(1E,1'E)-(2-Oxocyclopentane-1,3-diylidene)-bis-(methan-1-yl-1-ylidene)-bis-(1-methylquinolinium) iodide (M2)

Following the method for production of **M1**, an orange solid **M2** (125 mg, 84%) was obtained. Mp >300 °C; ¹H NMR (400 MHz, D₂O) δ 9.11 (s, 2H), 9.05 (d, 2H, *J* = 7.9), 8.43 (s, 2H), 8.36 (s, 4H), 7.93 (s, 2H), 7.57 (s, 2H), 4.57 (s, 6H), 3.23 (s, 4H). ¹³C NMR (101 MHz, D₂O) δ 196.55, 153.10, 150.07, 144.16, 140.83, 139.58, 139.07, 133.98, 132.95, 132.10, 125.33, 122.49, 48.12, 28.71. ESI-HRMS *m/z*: calcd for C₂₇H₂₄N₂O [M–2I]²⁺ 196.0944, found 196.0943.

4.9. 6,6'-(1Z,1'Z)-(2-Oxocyclohexane-1,3-diylidene)-bis-(methan-1-yl-1-ylidene)-bis-(1-methylquinolinium) iodide (M3)

Following the method for production of **M1**, an orange solid **M3** (69 mg, 79%) was obtained. Mp >300 °C; ¹H NMR (400 MHz, DMSO-*d*₆) δ 9.52 (d, 2H, *J* = 5.6), 9.34 (d, 2H, *J* = 8.4), 8.68 (s, 2H), 8.57 (d, 2H, *J* = 9.2), 8.44 (d, 2H, *J* = 9.0), 8.22 (dd, 2H, *J* = 8.3, 5.8), 7.91 (s, 2H), 4.66 (s, 6H), 3.09 (d, 4H, *J* = 5.3), 1.93–1.74 (m, 2H). ESI-HRMS *m/z*: calcd for C₂₈H₂₆N₂O [M–2I]²⁺ 203.1023, found 203.1033.

4.10. 6,6'-(1E,1'E)-(1,1-Dimethyl-4-oxopiperidinium-3,5-diylidene)-bis-(methan-1-yl-1-ylidene)-bis-(1-methylquinolinium) iodide (M4)

Following the method for production of **M1**, an orange solid **M4** (90 mg, 72%) was obtained. Mp >300 °C; ¹H NMR (400 MHz, DMSO-*d*₆) δ 9.59 (d, 2H, *J* = 5.7), 9.40 (d, 2H, *J* = 8.4), 8.64 (d, 4H, *J* = 8.4), 8.43 (d, 2H, *J* = 9.5), 8.35 (s, 2H), 8.32–8.26 (m, 2H), 5.16 (s, 4H), 4.69 (s, 6H), 3.25 (s, 6H). ¹³C NMR (101 MHz, DMSO) δ 180.22, 151.20, 147.44, 139.80, 138.36, 136.86, 134.09, 131.70, 129.08, 127.98, 122.82, 119.79, 61.52, 51.81, 45.61. ESI-HRMS *m/z*: calcd for C₂₉H₃₀N₃O [M–3I+1]⁺ 437.2390, found 437.2315.

4.11. FRET assay

The oligonucleotide labeled with *FAM* and *TAMRA* (with *FAM*: 6-carboxyfluorescein and *TAMRA*: 6-carboxytetramethylrhodamine) was purchased from Invitrogen (China). After an initial dilution at 100 μ M concentration in purified water, further dilutions were carried out in the 10 mM Tris–HCl pH 7.4 and 60 mM KCl buffer. Fluorescence melting curves were determined with a Bio-Rad IQ5 real-time PCR machine, using a total reaction volume of 20 μ L, with 0.2 μ M of tagged oligonucleotide in a buffer containing 10 mM Tris–HCl pH 7.4 and 60 mM KCl. After a first equilibration step at 25 °C during 5 min, a stepwise increase of 1 °C every minute for 71 cycles to reach 95 °C was performed and measurements were made after each cycle with excitation at 492 nm and detection at 516 nm. The melting of the G-quadruplex was monitored alone or in the presence of various compounds and/or of double-stranded competitor ds26 as well as G-quadruplex competitor c-kit1, c-kit2, and HTG21. Final analysis of the data was carried out using Excel and Origin 6.0 (OriginLab Corp.).

4.12. ITC measurement

ITC measurements were carried out in a VP-ITC titration calorimeter (MicroCal, Northampton, MA). Before loading, the solutions were thoroughly degassed. The reference cell was filled with the degassed buffer. The preformed G-quadruplex DNA (5 μ M) was kept in the sample cell, and **M2** (400 μ M) in the same buffer was filled in the syringe of volume 300 μ L. **M2** solution was added sequentially in 10 μ L aliquots (for a total of 30 injections, 20 s duration each) at 4 min intervals at 25 °C. The heats of dilution were determined in parallel experiments by injecting **M2** solution of same concentration in the same buffer. The respective heats of dilution were subtracted from the corresponding binding experiments prior to curve fitting. The thermograms (integrated heat/injection data) obtained in ITC experiments were fit with proper model in Origin 6.0.

4.13. PCR stop assay

The PCR stop assay was conducted according to a modified protocol of the previous study.⁵⁴ The oligonucleotide Pu27 and the corresponding complementary sequence Pu27_{rev} were used here. The reactions were performed in 1 \times PCR buffer, containing with 10 pmol of each oligonucleotide, 0.16 mM dNTP, 2.5 U *Taq* polymerase, and the compounds to be tested. Reaction mixtures were incubated in a thermocycler with the following cycling conditions: 94 °C for 3 min, followed by 35 cycles of 94 °C for 30 s, 58 °C for 30 s, and 72 °C for 30 s. Amplified products were resolved on 15% non-denaturing polyacrylamide gels in 1 \times TBE and silver stained. IC₅₀ values were calculated using optical density read from Alpha-EaseFC software.

Acknowledgments

We thank the Natural Science Foundation of China (Grants U0832005, 90813011, 20772159, 30801436), the Ministry of Education of the People's Republic of China (Grant 200805581163), the Guangdong Natural Science Foundation (Grant 845100890 1000214), and the Science Foundation of Guangzhou (2009A1-E011-6) for financial support of this study.

Supplementary data

Supplementary data associated with this article can be found, in the online version, at doi:10.1016/j.bmc.2010.10.021.

References and notes

- Burge, S.; Parkinson, G. N.; Hazel, P.; Todd, A. K.; Neidle, S. *Nucleic Acids Res.* **2006**, *34*, 5402.
- Phan, A. T.; Kuryavyi, V.; Patel, D. J. *Curr. Opin. Struct. Biol.* **2006**, *16*, 288.
- Dai, J.; Carver, M.; Yang, D. *Biochimie* **2008**, *90*, 1172.
- Davis, J. T. *Angew. Chem., Int. Ed.* **2004**, *43*, 668.
- Henderson, E.; Hardin, C. C.; Walk, S. K.; Tinoco, L., Jr.; Blackburn, E. H. *Cell* **1987**, *51*, 899.
- Sen, D.; Gilbert, W. *Nature* **1988**, *334*, 364.
- Hanakahi, L. A.; Sun, H.; Maizels, N. J. *Biol. Chem.* **1999**, *274*, 15908.
- Simonsson, T.; Pecinka, P.; Kubista, M. *Nucleic Acids Res.* **1998**, *26*, 1167.
- Rankin, S.; Reszka, A. P.; Huppert, J.; Zloh, M.; Parkinson, G. N.; Todd, A. K.; Ladame, S.; Balasubramanian, S.; Neidle, S. *J. Am. Chem. Soc.* **2005**, *127*, 10584.
- Dexheimer, T. S.; Sun, D.; Hurley, L. H. *J. Am. Chem. Soc.* **2006**, *128*, 5404.
- Sun, D.; Guo, K.; Rusche, J. J.; Hurley, L. H. *Nucleic Acids Res.* **2005**, *33*, 6070.
- Huppert, J. L.; Balasubramanian, S. *Nucleic Acids Res.* **2005**, *33*, 2908.
- Du, Z.; Zhao, Y.; Li, N. *Nucleic Acids Res.* **2009**, *37*, 6784.
- Neidle, S. *Curr. Opin. Struct. Biol.* **2009**, *19*, 239.
- Ou, T.-M.; Lu, Y.-J.; Tan, J.-H.; Huang, Z.-S.; Wong, K.-Y.; Gu, L.-Q. *ChemMedChem* **2008**, *3*, 690.
- Stewart, S. A.; Weinberg, R. A. *Annu. Rev. Cell Dev. Biol.* **2006**, *22*, 531.
- Kim, N. W.; Piatyszek, M. A.; Prowse, K. R.; Harley, C. B.; West, M. D.; Ho, P. L.; Coviello, G. M.; Wright, W. E.; Weinrich, S. L.; Shay, J. W. *Science* **1994**, *266*, 2011.
- Masutomi, K.; Yu, E. Y.; Khurts, S.; Ben-Porath, I.; Currier, J. L.; Metz, G. B.; Brooks, M. W.; Kaneko, S.; Murakami, S.; DeCaprio, J. A.; Weinberg, R. A.; Stewart, S. A.; Hahn, W. C. *Cell* **2003**, *114*, 241.
- Neidle, S.; Parkinson, G. *Nat. Rev. Drug Discovery* **2002**, *1*, 383.
- De Cian, A.; Lacroix, L.; Douarre, C.; Temime-Smaali, N.; Trentesaux, C.; Riou, J.-F.; Mergny, J.-L. *Biochimie* **2008**, *90*, 131.
- Davis, T. L.; Firulli, A. B.; Kinniburgh, A. J. *Proc. Natl. Acad. Sci. U.S.A.* **1989**, *86*, 9682.
- Berberich, S. J.; Postel, E. H. *Oncogene* **1995**, *10*, 2343.
- Siddiqui-Jain, A.; Grand, C. L.; Bearss, D. J.; Hurley, L. H. *Proc. Natl. Acad. Sci. U.S.A.* **2002**, *99*, 11593.
- Sun, D.; Hurley, L. H. *J. Med. Chem.* **2009**, *52*, 2863.
- Brooks, T. A.; Hurley, L. H. *Nat. Rev. Cancer* **2009**, *9*, 849.
- Gonzalez, V.; Hurley, L. H. *Annu. Rev. Pharmacol. Toxicol.* **2010**, *50*, 111.
- Hurley, L. H. *Nat. Rev. Cancer* **2002**, *2*, 188.
- Neidle, S. *FEBS J.* **2010**, *277*, 1118.
- Monchaud, D.; Teulade-Fichou, M.-P. *Org. Biomol. Chem.* **2008**, *6*, 627.
- Tan, J.-H.; Gu, L.-Q.; Wu, J.-Y. *Mini-Rev. Med. Chem.* **2008**, *8*, 1163.
- Shin-ya, K.; Wierzbka, K.; Matsuo, K.-I.; Ohtani, T.; Yamada, Y.; Furihata, K.; Hayakawa, Y.; Seto, H. *J. Am. Chem. Soc.* **2001**, *123*, 1262.
- Moore, M. J. B.; Schultes, C. M.; Cuesta, J.; Cuenca, F.; Gunaratnam, M.; Taniou, F. A.; Wilson, W. D.; Neidle, S. *J. Med. Chem.* **2006**, *49*, 582.
- Dash, J.; Shirude, P. S.; Hsu, S.-T. D.; Balasubramanian, S. *J. Am. Chem. Soc.* **2008**, *130*, 15950.
- Mueller, S.; Pantos, G. D.; Rodriguez, R.; Balasubramanian, S. *Chem. Commun.* **2009**, 80.
- Gomez, D.; Aouali, N.; Renaud, A.; Douarre, C.; Shin-ya, K.; Tazi, J.; Martinez, S.; Trentesaux, C.; Morjani, H.; Riou, J.-F. *Cancer Res.* **2003**, *63*, 6149.
- De Cian, A.; Delemos, E.; Mergny, J.-L.; Teulade-Fichou, M.-P.; Monchaud, D. *J. Am. Chem. Soc.* **2007**, *129*, 1856.
- Pennarun, G.; Granotier, C.; Gauthier, L. R.; Gomez, D.; Hoffschir, F.; Mandine, E.; Riou, J.-F.; Mergny, J.-L.; Mailliet, P.; Boussin, F. D. *Oncogene* **2005**, *24*, 2917.
- Adams, B. K.; Ferstl, E. M.; Davis, M. C.; Herold, M.; Kurtkaya, S.; Camalier, R. F.; Hollingshead, M. G.; Kaur, G.; Sausville, E. A.; Rickles, F. R.; Snyder, J. P.; Liotta, D. C.; Shoji, M. *Bioorg. Med. Chem.* **2004**, *12*, 3871.
- Mergny, J.-L.; Lacroix, L.; Teulade-Fichou, M.-P.; Hounsou, C.; Guittat, L.; Hoarum, M.; Arimondo, P. B.; Vigneron, J.-P.; Lehn, J.-M.; Riou, J.-F.; Garestier, T.; Helene, C. *Proc. Natl. Acad. Sci. U.S.A.* **2001**, *98*, 3062.
- Dash, J.; Shirude, P. S.; Balasubramanian, S. *Chem. Commun.* **2008**, 3055.
- Tan, J.-H.; Ou, T.-M.; Hou, J.-Q.; Lu, Y.-J.; Huang, S.-L.; Luo, H.-B.; Wu, J.-Y.; Huang, Z.-S.; Wong, K.-Y.; Gu, L.-Q. *J. Med. Chem.* **2009**, *52*, 2825.
- Moorhouse, A. D.; Santos, A. M.; Gunaratnam, M.; Moore, M.; Neidle, S.; Moses, J. E. *J. Am. Chem. Soc.* **2006**, *128*, 15972.
- Shirude, P. S.; Gillies, E. R.; Ladame, S.; Godde, F.; Shin-ya, K.; Huc, I.; Balasubramanian, S. *J. Am. Chem. Soc.* **2007**, *129*, 11890.
- Sparapani, S.; Haider, S. M.; Doria, F.; Gunaratnam, M.; Neidle, S. *J. Am. Chem. Soc.* **2010**, *132*, 12263.
- Doyle, M. L. *Curr. Opin. Biotechnol.* **1997**, *8*, 31.
- Pagano, B.; Giancola, C. *Curr. Cancer Drug Targets* **2007**, *7*, 520.
- Pagano, B.; Mattia, C. A.; Giancola, C. *Int. J. Mol. Sci.* **2009**, *10*, 2935.
- Martino, L.; Virno, A.; Pagano, B.; Virgilio, A.; Di Micco, S.; Galeone, A.; Giancola, C.; Bifulco, G.; Mayol, L.; Randazzo, A. *J. Am. Chem. Soc.* **2007**, *129*, 16048.
- Pagano, B.; Virno, A.; Mattia, C. A.; Mayol, L.; Randazzo, A.; Giancola, C. *Biochimie* **2008**, *90*, 1224.
- Sun, T.; Zhang, Y. *Nucleic Acids Res.* **2008**, *36*, 1654.
- Phan, A. T.; Kuryavyi, V.; Burge, S.; Neidle, S.; Patel, D. J. *J. Am. Chem. Soc.* **2007**, *129*, 4386.
- Phan, A. T.; Kuryavyi, V.; Gaw, H. Y.; Patel, D. J. *Nat. Chem. Biol.* **2005**, *1*, 167.
- Neidle, S.; Parkinson, G. N. *Biochimie* **2008**, *90*, 1184.
- Ou, T.-M.; Lu, Y.-J.; Zhang, C.; Huang, Z.-S.; Wang, X.-D.; Tan, J.-H.; Chen, Y.; Ma, D.-L.; Wong, K.-Y.; Tang, J. C.-O.; Chan, A. S.-C.; Gu, L.-Q. *J. Med. Chem.* **2007**, *50*, 1465.
- Wang, X.-D.; Ou, T.-M.; Lu, Y.-J.; Li, Z.; Xu, Z.; Xi, C.; Tan, J.-H.; Huang, S.-L.; An, L.-K.; Li, D.; Gu, L.-Q.; Huang, Z.-S. *J. Med. Chem.* **2010**, *53*, 4390.
- Lemarteleur, T.; Gomez, D.; Paterski, R.; Mandine, E.; Mailliet, P.; Riou, J.-F. *Biochem. Biophys. Res. Commun.* **2004**, *323*, 802.